Int. J. Electrochem. Sci., 15 **(2020)** 526 – 534, doi: 10.20964/2020.01.77

International Journal of
ELECTROCHEMICAL
SCIENCE
www.electrochemsci.org

Complex Hollow Structures of Cobalt(II) Sulfide as a Cathode for Lithium–Sulfur Batteries

Miaomiao Li [2], *Wangjun Feng*[1,2*], *Xuan Wang* [1,2*]

[1] State Key Laboratory of Advanced Processing and Recycling Nonferrous Metals, Lanzhou University of Technology, Lanzhou 730050, China;
[2] School of Science, Lanzhou University of Technology, Lanzhou 730050, China
[*]E-mail: wjfeng@lut.cn, wangxuan2010@lut.cn

Received: 8 September 2019 / *Accepted:* 9 November 2019 / *Published:* 30 November 2019

Lithium-sulfur batteries are considered the most promising candidates in the next generation of electrochemical energy storage because of their huge advantages in energy density, coulombic efficiency and price. One of the problems to be solved is promoting the conversion of polysulfides while maintaining high sulfur utilization. Complex double-layered hollow nanostructures have attracted wide attention as battery cathode materials. A ZIF-67 nanocube is used as a template to form a double-layer hollow structure (denoted as CoS) in which the inner layer is a CoS nanobox and the outer shell is a CoS nanosheet. In general, the double-layer hollow structure not only maximizes the encapsulation of sulfur but also provides sufficient reaction sites to optimize the electrochemical properties of the material. As a cathode material for Li–S batteries, cobalt-based sulfides also improve electrochemical performance due to their high electronic conductivity and abundance of redox reaction sites. The initial discharge capacity of the battery at 0.1 C was 1275.76 mA h g^{-1}, demonstrating excellent rate performance.

Keywords: Lithium–sulfur batteries; ZIF-67 nanocube; double-layer hollow structure; cathode

1. INTRODUCTION

A high theoretical capacity (1675 mA h g^{-1}) and the low cost of nontoxic sulfur make lithium sulfur batteries widely sought after, but their industrial application still faces many challenges. First, the insulating properties of sulfur and its discharge products (Li_2S_2/Li_2S) lead to a decrease in specific capacity. Second, polysulfide dissolution and shuttle effects lead to a loss of active materials, poor cycling stability and low coulombic efficiency. In addition, a large volume change in the process of charging and discharging leads to serious capacity attenuation [1-3].

To address these problems, metal organic frameworks (MOFs) have become potential host materials, which are porous materials formed by a self-assembly of organic ligands and metal ions through coordination bonds. They have a large specific surface area, an adjustable porous structure and a designable pore surface [4-6]. With the advancement of MOF research, a variety of redox active MOFs have been synthesized by reasonably selecting electroactive metal ions or organic functional groups. MOF-related materials also include MOFs, MOF composites and MOF-derived materials; moreover, MOF-derived materials obtained by using MOFs as self-sustaining templates have broad applications. The complex hollow structure derived from a metal-organic framework is widely used in the battery field due to its unique structural characteristics and attractive chemical properties. These materials have low density, high pore volume and short charge transport length. In lithium-sulfur (Li–S) batteries, this unique structure is capable of storing large amounts of sulfur, adapting to changes in the volume of sulfur during cycling, and avoiding the dissolution of discharge products [7,8]. The complex hollow structure of Co-based sulfides derived from the metal-organic framework is an excellent sulfur host material due to its high electron conductivity and abundant redox reaction sites. It has been discovered that some sulfides with polar surfaces can form strong chemical bonds with lithium polysulfide species [9,10]. Thus, metal sulfides have high theoretical capacity due to the above advantages and have attracted widespread attention as advanced cathode materials for batteries.

Here, we synthesize a double-shell hollow CoS nanomaterial as a new sulfur host for lithium-sulfur batteries. A template provided by ZIF-67 nanocubes with Na_2S and a sequential reaction with water and Na_2S results in a formation of single-shell hollow cubes assembled with CoS-nanoparticles and CoS-nanosheets. The double-layer hollow structure not only encapsulates sulfur to a great extent but also chemically combines with polysulfide to suppress its shuttle effect. When used in lithium-sulfur batteries as cathode materials, it exhibits good electrochemical performance [11,12].

2. EXPERIMENTAL

2.1 Synthesis of ZIF-67 nanocubes

The ZIF-67 nanocubes were synthesized according to a typical experiment [13]. The specific steps are as follows. First, 580 mg $Co(NO_3)_2•6H_2O$ was dissolved in 20 mL of water containing 10 mg of CTAB. Then, the cobalt-containing solution was rapidly poured into 140 mL of water containing 9.08 g of 2-methylimidazole under magnetic stirring. After stirring for 20 min, the precipitate was collected by centrifugation, washed several times with water and dried overnight to obtain a purple powder.

2.2 Synthesis of CoS

The purple powder was dispersed in 20 mL ethanol by sonication. After adding 5 mL of deionized water, it was heated in an oil bath at 85 °C for a while. Then, 5 ml of ethanol solution containing 100 mg of Na_2S was added, and heating was continued for an additional two hours. The

products were collected by centrifugation, washed 3 times with water and dried at 70 °C overnight to obtain a double-layer hollow structure of CoS [14].

2.3 Materials characterization

The crystal phase was determined by X-ray powder diffraction (XRD; Rigaku, D8-Advance X-ray Diffractometer) with a scanning range of 10° to 90°. The morphology of the products was analyzed using scanning electron microscopy (SEM; JSM-6700F) at 20 kV and transmission electron microscopy (TEM; JEM-2100F). The elemental mapping was recorded using energy-dispersive X-ray spectroscopy (EDX) attached to a scanning electron microscope (SEM) [15].

2.5 Cell assembly and electrochemical measurements

To prepare the electrodes, CoS/S, Super P, and PVDF binder were mixed in N-methyl-l-2-pyrrolidone with a mass ratio of 7:2:1. Then, the slurry was applied uniformly onto an aluminum foil and dried in a vacuum oven at 55 °C for 12 h to obtain an electrode film. Next, the cathode film was cut into round disks with a diameter of 9 mm. The 2025-type coin cells were assembled using a Celgard 2400 membrane as the separator and 15.8 mm of lithium foil as the anode. The electrolyte was composed of 1 M lithium hexafluorophosphate (LiTFSI) in a mixture of 1,3-dioxolane (DOL) and dimethoxymethane (DME) (1:1, v/v) with 2 wt% $LiNO_3$. Galvanostatic discharge-charge tests were conducted using a LAND-CT2001A instrument (Wuhan, China) within a voltage range of 2.8-1.7 V. The CV and EIS measurements of the battery were taken using a CS350 electrochemical workstation (Corrtest, China) with a scanning range of 1.7-2.8 V and a scanning rate of 0.1 mV s^{-1} [16,17].

3. RESULTS AND DISCUSSION

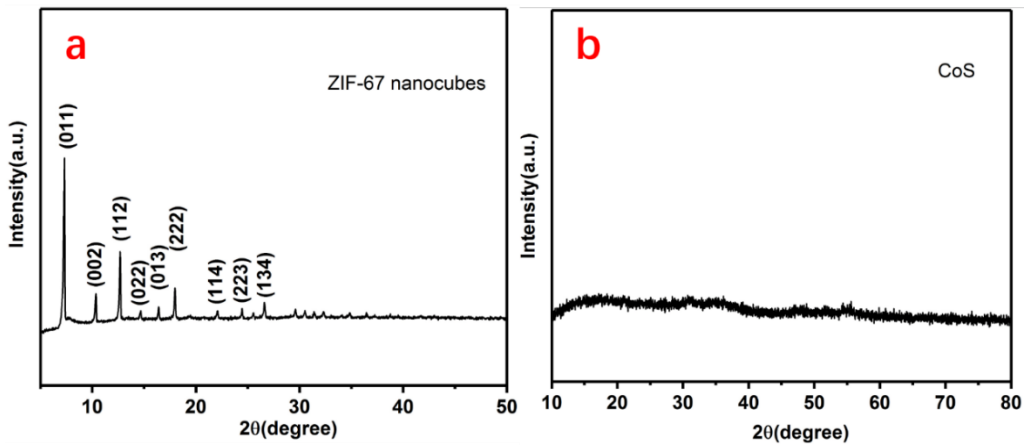

Figure 1. (a) XRD characterization of the ZIF-67 nanocubes and (b) XRD characterization of CoS.

ZIF-67 nanocubes are synthesized by mixing 2-methylimidazole and a $Co(NO_3)_2$ aqueous solution with an appropriate amount of cetyltrimethylammonium bromide (CTAB). The crystallographic phases of the ZIF-67 nanocubes were analyzed using XRD. As shown in Fig. 1a, typical diffraction peaks of the (011), (002), (112), and (222) planes are shown, demonstrating that the ZIF-67 crystal has been successfully synthesized. Comparing the XRD patterns of CoS with those in the existing literature verifies that CoS has been successfully synthesized [18].

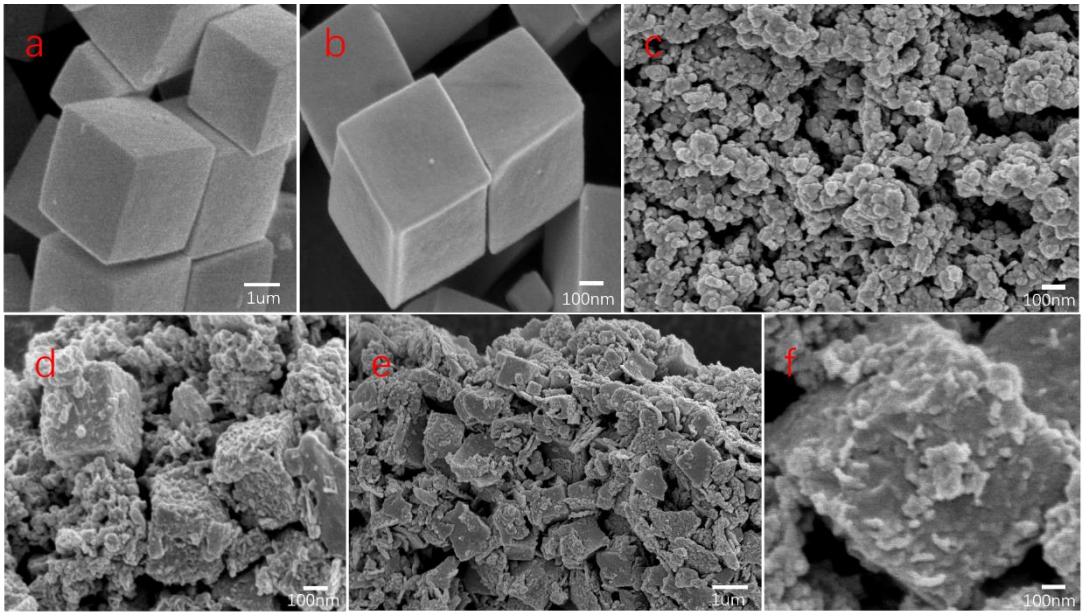

Figure 2. (a) (b) SEM images of the ZIF-67 nanocubes. (c-f) SEM image of CoS with different heating times.

Studies have shown that the addition of CTAB changes the growth rate of different faces and forms uniform ZIF-67 nanocubes. SEM images of the ZIF-67 nanocubes are shown in Fig. 2a and Fig. 2b. Each synthesized ZIF-67 particle has a good cubic shape with a smooth surface and uniform distribution. The ZIF-67 nanocubes are subjected to a reflux reaction for a specified amount of time in a mixed solvent of ethanol and water followed by sulfidation under the action of Na_2S to synthesize a double-layered CoS hollow structure. During this process, the heating time must be strictly controlled after the addition of deionized water; otherwise, a completely hollow structure or a collapsed outer casing will be produced. In our experiments, different heating times were studied. Fig. 2c to 2f were heated for 30 min, 25 min, 20 min and 15 min, respectively. As seen from the figure, when the heating time is different, the morphology of the product changes greatly. Heating for an excessive amount of time causes the structure to collapse, thus, 15 min is chosen as the optimum heating time. It can be seen from Fig. 2f that the final product maintains the shape of the cube well [19,20].

The crystal ZIF-67 particles are converted into an amorphous structure mainly composed of Co and S at a molar ratio of 1:1.28, and the final energy spectrum (EDS) mapping shows that it is composed of CoS. TEM images of CoS obtained after heating for 20 min are shown in Fig. 3b to 3d. As seen from Fig. 3b, the obtained materials maintain the shape of the cube in general, but

unfortunately, the double-shell structure is unclear. Thus, it may be observed that the inner layer is a CoS nanoparticle and that the outer layer is a CoS nanosheet. The reason for the above analysis may be that the heating time is too long, causing the cube structure to partially collapse [21-24].

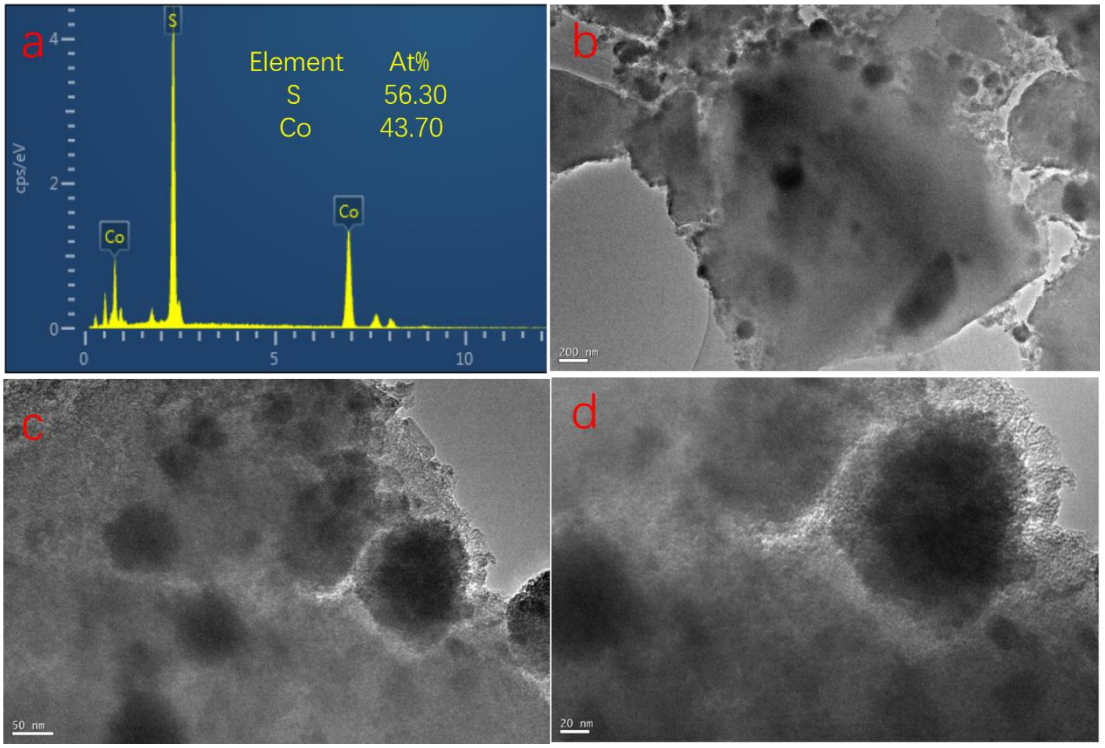

Figure 3. (a) EDX spectrum and (b) (c) (d) TEM images of CoS.

To verify the applicability of the double-layer hollow structure CoS in a Li-S battery, the electrochemical performance of the electrode material was evaluated. As shown in Fig. 4a, the charge and discharge curves of the CoS/S electrode materials at different rates were tested. At a rate current density of 0.1 C, 0.2 C and 0.5 C, the charge-discharge curve exhibits a typical two-plateau profile, which corresponds to the breakage and generation of S-S bonds between the active substances in the lithium-sulfur batteries, showing that a complex multiphase multistep reaction process involving electron ion transfer occurs. When the current density is 0.1 C (1.0 C = 1675 mAh g-1), the initial discharge capacity is 1275.76 mA h g^{-1}. However, no second platform was observed at high 1 C current densities. It is worth mentioning that as the current density increases from 0.1 C to 0.5 C, the discharge specific capacity of the electrode material attenuates rapidly by the second plateau at 2.1 V from 1275.8 mA h g-1 to 858.7 mA h g-1, but the specific discharge capacity from the first platform at 2.3 V is only reduced by 63.97 mA h g^{-1}. This phenomenon indicates that CoS is the sulfur host, and its main problem is that lithium polysulfide and Li_2S have certain difficulties in the conversion process; however, its complex structure has great advantages for inhibiting the shuttle effect of polysulfide. As shown in Table 1, the first discharge platform of the CoS electrode material contributes a greater specific capacity than that of other carrier materials [25-28]. As shown in Fig. 4b, when the discharge rate is increased from 0.1 C to 2 C, the discharge capacity gradually decreases, and the

discharge capacities of the electrodes at 0.1 C, 0.2 C, 0.5 C, 1 C and 2 C for 10 cycles are 1275.76, 1002.36, 858.73, 491.30 and 206.10 mA h g-1, respectively. When the current density returns to 0.1 C, the cathode still has a reversible capacity of 807.38 mAg^{-1}. The initial capacity is greatly restored, demonstrating that the rate performance of the CoS/S electrode is relatively stable. The main reason may be that the sulfur inside the pores cannot fully react at a higher current density. Moreover, the long cycle performance of the prepared sulfur electrode was also investigated, as shown in Fig. 4c. At a current density of 0.2 C, The CoS/S electrode shows an initial capacity of 1002 mAh g^{-1} and a capacity retention of 429 mAh g-1 after 200 cycles. The double-layer hollow CoS/S electrode has good electrochemical performance because the unique structure can effectively inhibit the dissolution and shuttle behavior of polysulfide, resulting in a high durability during Li-S electrochemistry. At the same time, the cubic hollow structure can buffer the volume change of sulfur during charge and discharge, effectively maintaining the structural stability of the electrode, and providing a rich electrode/electrolyte interface for fast and efficient electron/ion transport.

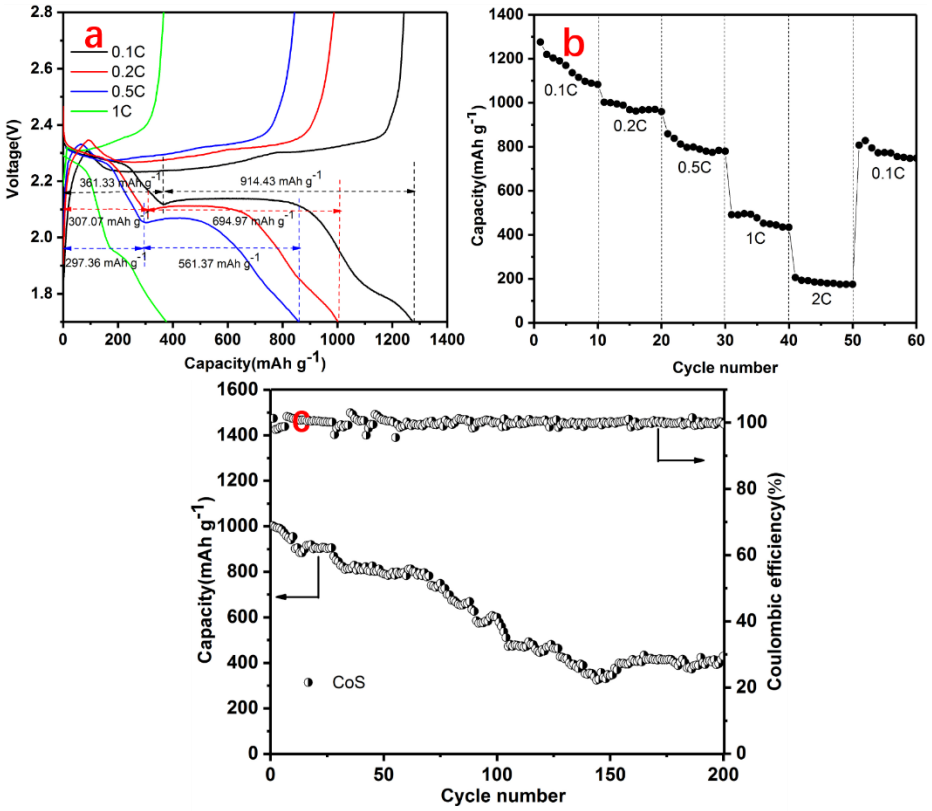

Figure 4. (a) Charge–discharge profiles of the CoS cathode at a rate current density of 0.1 C, 0.2 C, 0.5 C, and 1 C; (b) rate capability of the CoS cathode; and (c) long-term cycling performance of the CoS cathode at 0.2 C current density for 200 cycles.

Table 1. Contribution of different cathode materials to the specific capacity in lithium-sulfur batteries.

Sulfur host	Capacity of first plateau at 0.5 C (mAh g^{-1})	Capacity of second plateau at 0.5 C (mAh g^{-1})	Ref
RGO/C-Co	210	570	[25]
CH@LDH	250	300	[26]
Co@N−C	220	680	[27]
RGO@ZIF-67	200	590	[28]
N,S-codoped graphene	280	520	[29]
CoS	297.36	561.37	This work

To analyze the electrochemical performance of the CoS/S electrode, we collected cyclic voltammetry (CV) data for the first two cycles at a scan rate of 0.1 mV s^{-1} in a voltage range of 1.7 to 2.8 V, as shown in Fig. 5a. During the reduction process, the CoS/S cathode showed two pronounced peaks at approximately 2.25 V and 2.0 V. The peak value of 2.25 V corresponds to the reduction of elemental S to soluble lithium polysulfide (Li_2Sx, x=4-8), while the peak of 2.0 V is due to the reduction of lithium polysulfide (Li_2Sx, x=4-8) to insoluble Li_2S_2 and/or Li_2S [29-31]. Likewise, a peak appeared at approximately 2.39 V in the anodic scan, which is related to the oxidation of insoluble Li_2S_2/Li_2S to lithium polysulfide (Li_2Sx, x=4-8), and from lithium polysulfide (Li_2Sx, x=4-8) to elemental S [32, 33]. Fig. 5a shows that the liquid-solid conversion at 2.0 V is significantly reduced. The reduction peak area is small, and the polarization is severe, which is consistent with the electrochemical performance analysis of the electrode material.

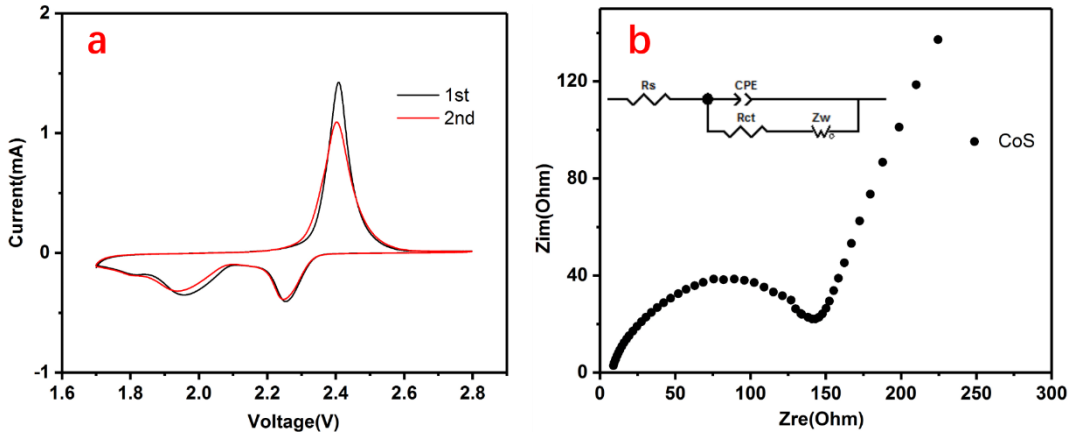

Figure 5. (a) The initial two CV curves of CoS and (b) Nyquist plots of CoS.

The electrochemical properties of the CoS samples were further studied by electrochemical impedance spectroscopy (EIS). The test results are shown in Fig. 5b, and the equivalent circuit

diagram for EIS data fitting is also given in the figure. As shown in Fig. 5b, the Nyquist plot of the CoS sample is semicircular in the high frequency region due to its electron transfer-limited process, and it is linear in the low frequency range due to the diffusion-limited process [34-37]. In general, charge transfer resistance (Rct) greatly affects the electrochemical performance of electrode materials. Thus, the low Rct value of CoS makes it a good prospective material for application in batteries [38, 39].

4. CONCLUSION

In summary, we use the unique reactivity of ZIF-67 to report a template-engaged formation of double-layer hollow structure CoS as a cathode material for lithium-sulfur batteries. The synthesis process is mainly the modulation of the reaction sequence of a ZIF-67 template with water and Na_2S. The complex hollow structure has a large surface area and suitable mesopores, which can improve the transport rate of the electrolyte and provide abundant active sites for the electrochemical reaction. In addition, the double-shell structure can trap the electrolyte between the shells and promote a redox reaction by providing a large driving force. The inner shell layer and the outer shell layer are connected to each other, have good structural robustness, and improve electrochemical stability. Due to these structural advantages, double-layer CoS exhibits excellent electrochemical performance as an electrode material. It is apparent from the CV curve and experimental results that it has good charge and discharge capacity, energy efficiency, and cycle stability.

ACKNOWLEDGEMENT
This work was financially supported by the National Natural Science Foundation of China (Grant No.11264023) and the HongLiu first-class disciplines Development Program of Lanzhou University of Technology.

References

1. Z. Li, C. Li, X. Ge, J. Ma, Z. Zhang, Q. Li, C. Wang, L. Yin, *Nano Energy*, 23 (2016) 15–26.
2. Y.-X. Wang, B. Zhang, W. Lai, Y. Xu, S.-L. Chou, H.-K. Liu, S.-X. Dou, *Advanced Energy Materials*, 7 (2017) 1602829.
3. J. Zhang, L. Yu, X.W.D. Lou, *Nano Research*, 10 (2017) 4298–4304.
4. X.-F. Wang, X.-Z. Song, K.-M. Sun, L. Cheng, W. Ma, *Polyhedron*, 152 (2018) 155–163.
5. Z. Zhang, Y. Chen, X. Xu, J. Zhang, G. Xiang, W. He, X. Wang, *Angewandte Chemie International Edition*, 53 (2014) 429–433.
6. S. Yang, L. Peng, E. Oveisi, S. Bulut, D.T. Sun, M. Asgari, O. Trukhina, W.L. Queen, *Chemistry - A European Journal*, 24 (2018) 4234–4238.
7. L. Zhou, Z. Zhuang, H. Zhao, M. Lin, D. Zhao, L. Mai, *Advanced Materials*, 29 (2017) 1602914.
8. H. Chen, M.Q. Wang, Y. Yu, H. Liu, S.-Y. Lu, S.-J. Bao, M. Xu, *ACS Applied Materials & Interfaces*, 9 (2017) 35040–35047.
9. J. Ren, Q. Meng, Z. Xu, X. Zhang, J. Chen, *Journal of Electroanalytical Chemistry*, 836 (2019) 30–37.

10. Z. Wang, L. Wang, S. Liu, G. Li, X. Gao, *Advanced Functional Materials*, 29 (2019) 1901051.
11. Y. Lu, L. Yu, M. Wu, Y. Wang, X.W.D. Lou, *Advanced Materials*, 30 (2018) 1702875.
12. J. Yan, Y. Huang, X. Han, X. Gao, P. Liu, *Composites Part B: Engineering*, 163 (2019) 67–76.
13. H. Hu, B.Y. Guan, X.W. (David) Lou, *Chem*, 1 (2016) 102–113.
14. J. Zhang, H. Hu, Z. Li, X.W.D. Lou, *Angewandte Chemie International Edition*, 55 (2016) 3982–3986.
15. Y. Cao, *Int. J. Electrochem. Sci*, (2017) 9084.
16. W. Su, *Int. J. Electrochem. Sci*, (2018) 6005.
17. C. Liang, X. Zhang, Y. Zhao, T. Tan, Y. Zhang, *Journal of Solid State Electrochemistry*, 23 (2019) 565–572.
18. W. Cai, G. Li, D. Luo, G. Xiao, S. Zhu, Y. Zhao, Z. Chen, Y. Zhu, Y. Qian, *Advanced Energy Materials*, 8 (2018) 1802561.
19. R. Zhao, Z. Liang, R. Zou, Q. Xu, *Joule*, 2 (2018) 2235–2259.
20. H. Hu, L. Han, M. Yu, Z. Wang, X.W. (David) Lou, *Energy & Environmental Science*, 9 (2016) 107–111.
21. Y.-X. Mo, J.-X. Lin, Y.-J. Wu, Z.-W. Yin, Y.-Q. Lu, J.-T. Li, Y. Zhou, T. Sheng, L. Huang, S.-G. Sun, *ACS Applied Materials & Interfaces*, 11 (2019) 4065–4073.
22. J. Cai, C. Wu, Y. Zhu, K. Zhang, P.K. Shen, *Journal of Power Sources*, 341 (2017) 165–174.
23. C. Song, *Int. J. Electrochem. Sci*., 14 (2019) 2372–2382.
24. L. Chen, *Int. J. Electrochem. Sci*., 14 (2019) 2846–2856.
25. Z. Li, C. Li, X. Ge, J. Ma, Z. Zhang, Q. Li, C. Wang, L. Yin, *Nano Energy*, 23 (2016) 15–26.
26. J. Zhang, H. Hu, Z. Li, X.W.D. Lou, *Angew. Chem. Int. Ed*., 55 (2016) 3982–3986.
27. Y. Li, J. Fan, J. Zhang, J. Yang, R. Yuan, J. Chang, M. Zheng, Q. Dong, *ACS Nano*, 11 (2017) 11417–11424.
28. Q. Pang, L.F. Nazar, *ACS Nano*, 10 (2016) 4111–4118.
29. G. Zhou, E. Paek, G.S. Hwang, A. Manthiram, *Nat Commun*, 6 (2015) 7760.
30. Z. Wang, S. Zhang, L. Zhang, R. Lin, X. Wu, H. Fang, Y. Ren, *Journal of Power Sources*, 248 (2014) 337–342.
31. J. Zhang, X. Yan, J. Zhang, W. Cai, Z. Wu, Z. Zhang, *Journal of Power Sources*, 198 (2012) 223–228.
32. R. Fang, S. Zhao, Z. Sun, D.-W. Wang, H.-M. Cheng, F. Li, *Advanced Materials*, 29 (2017) 1606823.
33. J. Wang, S. Li, Y. Zhao, J. Shi, L. Lv, H. Wang, Z. Zhang, W. Feng, *RSC Advances*, 8 (2018) 6660–6666.
34. Z. Li, H.B. Wu, X.W. (David) Lou, *Energy & Environmental Science*, 9 (2016) 3061–3070.
35. H. Jia, Z. Wang, X. Zheng, Y. Cai, J. Lin, H. Liang, J. Qi, J. Cao, J. Feng, W. Fei, Ele*ctrochimica Acta*, 312 (2019) 54–61.
36. M. Li, W. Feng, W. Su, C. Song, L. Cheng, *Ionics*, 25 (2019) 4037–4045.
37. M. Li, W. Feng, W. Su, X. Wang, *Journal of Solid State Electrochemistry*, 23 (2019) 2317–2324.
38. K.D. Ikkurthi, S. Srinivasa Rao, M. Jagadeesh, A.E. Reddy, T. Anitha, H.-J. Kim, *New Journal of Chemistry*, 42 (2018) 19183–19192.
39. M. Li, W. Feng, W. Su, C. Song, L. Chen, *Integrated Ferroelectrics*, 200 (2019) 82–89.